4-Amido-2-aryl-1,2,4-triazolo[4,3-*a*]quinoxalin-1-ones as New Potent and Selective Human A_3 Adenosine Receptor Antagonists. Synthesis, Pharmacological Evaluation, and Ligand−Receptor Modeling Studies

Ombretta Lenzi,[†] Vittoria Colotta,*[,†] Daniela Catarzi,[†] Flavia Varano,[†] Guido Filacchioni,[†] Claudia Martini,[‡] Letizia Trincavelli,[‡] Osele Ciampi,[‡] Katia Varani,[§] Federico Marighetti,[#] Erika Morizzo,[#] and Stefano Moro[#]

Dipartimento di Scienze Farmaceutiche, Laboratorio di Progettazione, Sintesi e Studio di Eterocicli Biologicamente Attivi, Università di Firenze, Polo Scientifico, Via Ugo Schiff, 6, 50019 Sesto Fiorentino, Italy, Dipartimento di Psichiatria, Neurobiologia, Farmacologia e Biotecnologie, Università di Pisa, Via Bonanno, 6, 56126 Pisa, Italy, Dipartimento di Medicina Clinica e Sperimentale, Sezione di Farmacologia, Università di Ferrara, Via Fossato di Mortara 17-19, 44100 Ferrara, Italy, and Molecular Modeling Section, Dipartimento di Scienze Farmaceutiche, Università di Padova, Via Marzolo 5, 35131, Padova, Italy

Received March 30, 2006

A structural investigation on some 4-amido-2-phenyl-1,2-dihydro-1,2,4-triazolo[4,3-*a*]quinoxalin-1-one derivatives, designed as human A_3 adenosine receptor (hA_3 AR) antagonists, is described. In the new derivatives, some acyl residues with different steric bulk were introduced on the 4-amino group, and their combination with the 4-methoxy group on the 2-phenyl moiety, and/or the 6-nitro/6-amino substituent on the fused benzo ring, was also evaluated. Most of the new derivatives were potent and selective hA_3 AR antagonists. SAR analysis showed that hindering and lipophilic acyl moieties not only are well tolerated but even ameliorate the hA_3 affinity. Interestingly, the 4-methoxy substituent on the appended 2-phenyl moiety, as well as the 6-amino group, always exerted a positive effect, shifting the affinity toward the hA_3 receptor subtype. In contrast, the 6-nitro substituent exerted a variable effect. An intensive molecular modeling investigation was performed to rationalize the experimental SAR findings.

Introduction

Adenosine is a ubiquitous neuromodulator that elicits a wide variety of physiological effects by activating four different receptors, classified as A_1, A_{2A}, A_{2B}, and A_3 subtypes, belonging to the G-protein-coupled receptor superfamily.[1,2] All four adenosine receptors (ARs) have been cloned from different species[1] and pharmacologically characterized, the most recently being the A_3 subtype.[3] AR subtypes are differently coupled with adenylyl cyclase: A_1 and A_3 AR activation inhibits adenylyl cyclase, thus decreasing cAMP production, while A_{2A} and A_{2B} AR stimulation activates adenylyl cyclase and increases cAMP levels.[1] Activation of the A_3 AR is also associated with phospholipase C[4] and D[5] stimulation. The A_3 AR is widely distributed in mammals, but pronounced differences in expression levels between species exist.[6] In humans, the highest density of this receptor subtype has been found in lung and liver, with lower levels in aorta, brain, and testes.[6] The A_3 AR is involved in many important physiological effects of adenosine: modulation of cerebral and cardiac ischemic damage,[6,7] inflammation,[8,9] regulation of normal and tumor cell growth.[10,11] Accordingly, A_3 AR selective antagonists are being investigated as neuroprotective agents[12,13] and as potential drugs for the treatment of asthma and chronic obstructive pulmonary disease.[8,9]

Over the past decade, we have focused a part of our research on the study of AR antagonists belonging to strictly correlated classes of tricyclic compounds.[14−23] One of these classes is represented by the 4-amino-2-aryl-1,2,4-triazolo[4,3-*a*]quinoxalin-1-one derivatives, which were intensively investigated by evaluating the effect of different substituents on the 4-amino group, the 2-phenyl ring, and the fused benzo ring (Chart 1).[15,17−21] These studies led to the identification of some groups that, introduced one by one in a suitable position of the 1,2,4-triazolo[4,5-*a*]quinoxalin-1-one scaffold, afforded high A_3 AR affinity and good selectivity. These groups are acyl residues, such as the acetyl or benzoyl groups, on the 4-amino group (compounds **A** and **B**),[17] the para methoxy substituent on the 2-phenyl ring (compound **C**),[17] and the 6-nitro group (compound **D**).[18] In particular, the para methoxy and the 6-nitro group significantly enhanced the hA_3 selectivity of the ligands. Combination of these latter substituents (compound **E**) was also achieved, and it afforded nanomolar A_3 AR affinity and increased A_3 selectivity, with respect to that obtained by single substitution.[21] Molecular modeling studies were also carried out on these derivatives, and in a recent paper, we depicted the putative transmembrane binding motif of this class of antagonists on a model of the hA_3 AR.[21] Ligand−receptor modeling studies pointed out that (i) several hydrogen-bonding interactions seem to occur in the anchoring of these derivatives at the receptor site and some interactions involve the 1-oxo, 6-nitro, and 4-amino groups and (ii) both the 2-aryl and the fused benzo rings interact with two size-limited binding pockets and, as a consequence, the volume of the whole molecule is critical in fitting with the receptor. Because of the interesting binding profile, we decided to continue the structural investigation of this class of derivatives with the objective of optimizing the substitution of the 2-phenyl-1,2,4-triazolo[4,3-*a*]quinoxalin-1-one framework and, as a consequence, of gaining more insight about the structural requirements of the hA_3 AR binding cavity. Thus, we planned the synthesis of the novel triazoloquinoxalines **1**−**23**, which are depicted in Chart 2. The new compounds bear, on the 4-amino group, some acyl substituents with different steric bulk (acetyl (**1**−**5**), benzoyl (**6**−**11**), diphenylacetyl (**12**−**18**), two benzoyl residues (**19**−**23**)) and profitable substituents at key positions R_1 (OMe) and/or R_6 (NO_2). The decision to

* To whom correspondence should be addressed. Phone: +39 55 4573731. Fax: +39 55 4573780. E-mail: vittoria.colotta@unifi.it.
[†] Università di Firenze.
[‡] Università di Pisa.
[§] Università di Ferrara.
[#] Università di Padova.

10.1021/jm060373w CCC: $33.50
Published on Web 06/03/2006

Chart 1. Previously Reported 4-Amino-1,2,4-triazolo[4,3-*a*]quinoxalin-1-one Derivatives

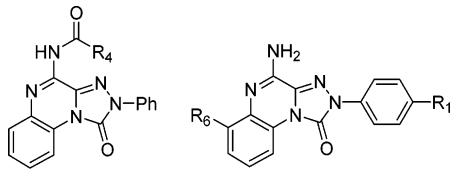

Chart 2. Hereby Reported 4-Amido-1,2,4-triazolo[4,3-*a*]quinoxalin-1-one Derivatives

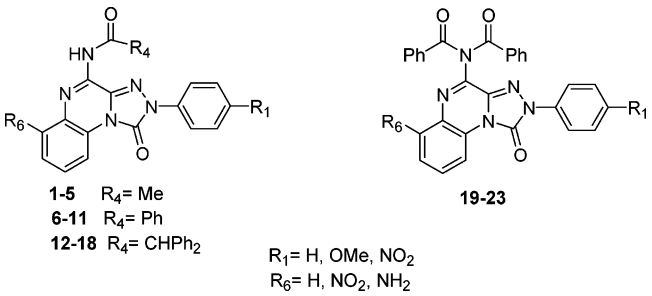

examine the hindering diphenylacetyl moiety (compounds **12**−**18**) as well as the two benzoyl residues (compounds **19**−**23**) was made because these substitutions had not yet been investigated in this class of AR antagonists. In some derivatives, the 6-nitro group was replaced by the 6-amino group, since previous data indicated that the presence of this latter also afforded nanomolar hA_3 AR affinity.[18,21] Furthermore, the effect of a nitro group at the R_1-position was evaluated. All these structural modifications, which increase the volume of the molecule, have provided information about the steric requirements of the receptor site and in particular about the space availability of the pocket where the R_4 substituent is accommodated. Molecular docking of these derivatives has been used to further refine our hA_3 AR receptor model.

Chemistry

The target derivatives **1**−**23** were prepared as depicted in Schemes 1 and 2. The starting 4-amino-2-aryl-1,2,4-triazolo-[4,3-*a*]quinoxalin-1-one derivatives **C**,[17] **D**,[18] **E**,[21] **24**,[21] and **25**[17] were prepared as previously reported.

The 4-acetamidotriazoloquinoxalin-1-one derivatives **1**−**3** were obtained under different experimental conditions. The 4-acetamido-2-(4-methoxyphenyl)-1,2,4-triazolo[4,3-*a*]quinoxalin-1-one **1** was prepared by stirring at room temperature a mixture of the 4-amino compound **C** and acetyl chloride in methylene chloride in the presence of pyridine. The synthesis of the 4-acetamido-6-nitro-2-phenyltriazoloquinoxalin-1-one **2** was achieved by reaction of the corresponding 4-amino compound **D** with acetic anhydride in dimethylformamide at room temperature and in the presence of 4-(dimethylamino)pyridine and triethylamine. The 4-acetamido-2-(4-methoxyphenyl)-6-nitro-1,2,4-triazolo[4,3-*a*]quinoxalin-1-one **3** was obtained from the corresponding 4-amino derivative **E** and acetyl chloride in refluxing anhydrous pyridine. Catalytic reduction (10% Pd/C) of the 6-nitro derivatives **2** and **3** in a Parr apparatus gave the corresponding 6-amino compounds **4** and **5**. The 4-benzamidotriazoloquinoxalin-1-one derivatives **6**, **8**, and **9** were synthesized by reaction of the corresponding 4-amino compounds **C**, **D**, and **E** with benzoyl chloride under the conditions described above to prepare derivative **1**. The synthesis of

Scheme 1[a]

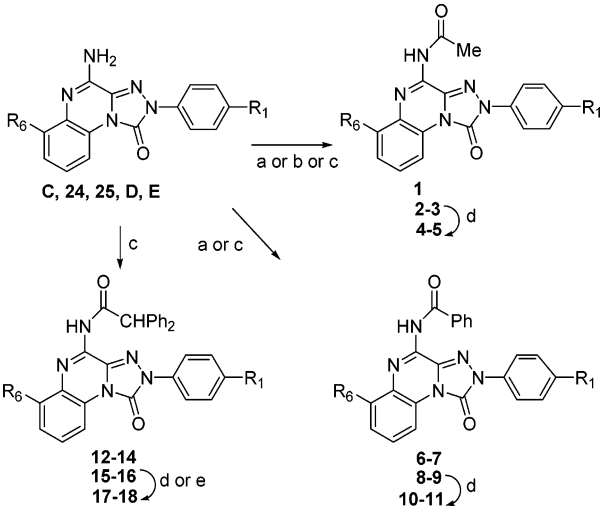

		R_1	R_6
C,	**1, 6, 12**	OMe	H
24,	**7, 13**	NO_2	H
25,	**14**	H	H
D,	**2, 8, 15**	H	NO_2
E,	**3, 9, 16**	OMe	NO_2
	4, 10, 17	H	NH_2
	5, 11, 18	OMe	NH_2

[a] (a) RCOCl, anhydrous CH_2Cl_2 and pyridine; (b) Ac_2O, 4-(dimethylamino)pyridine, Et_3N, anhydrous DMF; (c) RCOCl, anhydrous pyridine; (d) H_2, 10% Pd/C, DMF; (e) H_2, 10% Pd/C, EtOAc.

Scheme 2[a]

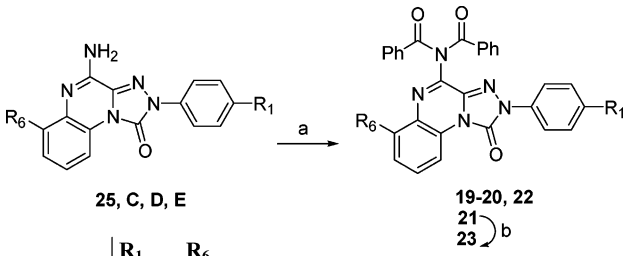

	R_1	R_6
25, 19	H	H
C, 20	OMe	H
D, 21	H	NO_2
E, 22	OMe	NO_2
23	H	NH_2

[a] (a) PhCOCl, anhydrous pyridine; (b) H_2, 10% Pd/C, EtOAc.

4-benzamido-2-(4-nitrophenyl)triazoloquinoxalin-1-one derivative **7** was instead performed from the corresponding 4-amino compound **24** and benzoyl chloride, which were reacted under the same conditions employed to obtain compound **3**. Catalytic reduction (10% Pd/C) of the 6-nitro derivatives **8** and **9** yielded the corresponding 6-amino compounds **10** and **11**. The 2-aryl-4-diphenylacetamidotriazoloquinoxalin-1-one derivatives **12**−**16** were obtained by allowing the 4-amino derivatives **C**, **24**, **25**, **D**, and **E** to react with diphenylacetyl chloride in boiling anhydrous pyridine, as described above for compound **3**. The 6-nitro derivatives **15** and **16** were transformed into the corresponding 6-amino derivatives **17** and **18** by catalytic hydrogenation (10% Pd/C) in a Parr apparatus. Finally, the 4-dibenzamido-2-aryltriazoloquinoxalin-1-ones **19**−**22** (Scheme 2) were synthesized after treatment of the 4-amino derivatives **25** and **C**−**E** with an excess of benzoyl chloride in refluxing anhydrous pyridine. The 6-nitro derivative **21** was catalytically reduced to the corresponding 6-amino compound **23**.

Table 1. Binding Activity at Human A_1, A_{2A}, A_3, and Bovine A_1 and A_{2A} ARs

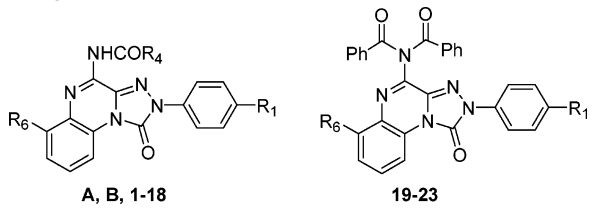

				K_i [a] (nM) or *I* (%)				
	R_4	R_1	R_6	hA_3[b]	hA_1[c]	hA_{2A}[d]	bA_1[e]	bA_{2A}[f]
A[g]	CH_3	H	H	2.0 ± 0.11	2000 ± 140	22%	4.3 ± 0.38	70%
1	CH_3	OMe	H	35.7 ± 2.40	34%	6%	245 ± 23.1	0%
2	CH_3	H	NO_2	18%			6 ± 0.55	36%
3	CH_3	OMe	NO_2	36%			0%	7%
4	CH_3	H	NH_2	48 ± 2.10	32%	367 ± 24	1 ± 0.09	6250 ± 410
5	CH_3	OMe	NH_2	5.5 ± 0.23	2700 ± 150	1100 ± 10	363 ± 24	20%
B[g]	Ph	H	H	1.47 ± 0.11	87.8 ± 6.30	88.2 ± 5.80	89.6 ± 7.20	53%
6	Ph	OMe	H	2.9 ± 0.30	37%	3585 ± 224	1010 ± 112	23%
7	Ph	NO_2	H	100 ± 9.60			55%	26%
8	Ph	H	NO_2	22 ± 2.60	15%	25%	32%	0%
9	Ph	OMe	NO_2	217 ± 20.40			35%	15%
10	Ph	H	NH_2	22 ± 1.70	98 ± 7.40	4850 ± 330	42 ± 3.1	27.8%
11	Ph	OMe	NH_2	1 ± 0.30	45%	24%	393 ± 27	16%
12	$CHPh_2$	OMe	H	44 ± 3.10	25%	27%	7.2 ± 0.41	28.5%
13	$CHPh_2$	NO_2	H	13%			30%	0%
14	$CHPh_2$	H	H	0.81 ± 0.03	18.8 ± 1.20	58%	10.2 ± 1.60	1160 ± 97.40
15	$CHPh_2$	H	NO_2	14.9 ± 1.10	12%	49%	3.9 ± 20.2	29.5%
16	$CHPh_2$	OMe	NO_2	0.8 ± 0.04	11%	2%	260 ± 11	0%
17	$CHPh_2$	H	NH_2	8.65 ± 0.61	2.5%	627 ± 34	1.6 ± 0.05	12%
18	$CHPh_2$	OMe	NH_2	2.58 ± 0.15	0%	31%	77.5 ± 5.20	0%
19		H	H	5.2 ± 0.31	1%	43%	30 ± 2.40	19%
20		OMe	H	3.29 ± 0.15	2%	26%	174.5 ± 11.40	6570 ± 460
21		H	NO_2	27%			39%	0%
22		OMe	NO_2	343 ± 21.0			20%	0%
23		H	NH_2	1243 ± 115			79 ± 5.10	36%
theophylline				86000 ± 7800	6200 ± 530	7900 ± 630	3800 ± 340	21000 ±1800
DPCPX				1300 ± 125	3.2 ± 0.2	260 ± 18	0.5 ± 0.03	337 ± 28

[a] The K_i values are the mean ± SEM of four separate assays, each performed in triplicate. [b] Displacement of specific [^{125}I]AB-MECA binding at human A_3 receptors expressed in CHO cells or percentage of inhibition (*I*) of specific binding at 1 μM. [c] Displacement of specific [^{3}H]DPCPX binding at hA_1 receptors expressed in CHO cells or percentage of inhibition (*I*) of specific binding at 10 μM. [d] Displacement of specific [^{3}H]NECA binding at hA_{2A} receptors expressed in CHO cells or percentage of inhibition (*I*) of specific binding at 10 μM. [e] Displacement of specific [^{3}H]DPCPX binding in bovine brain membranes or percentage of inhibition (*I*) of specific binding at 10 μM. [f] Displacement of specific [^{3}H]CGS 21680 binding from bovine striatal membranes or percentage of inhibition (*I*) of specific binding at 10 μM. [g] bA_1, bA_{2A}, hA_3 binding data were reported in ref 17.

Biochemistry

Compounds **1**−**23** were tested for their ability to displace [^{3}H]1,3-dipropyl-8-cyclopentylxanthine ([^{3}H]DPCPX) from A_1 AR in bovine cerebral cortical membranes, [^{3}H]2-[4-(2-carboxyethyl)phenethyl]amino-5′-(*N*-ethylcarbamoyl)adenosine ([^{3}H]-CGS 21680) from A_{2A} AR in bovine striatal membranes, and [^{125}I]N^6-(4-amino-3-iodobenzyl)-5′-(*N*-methylcarbamoyl)adenosine ([^{125}I]AB-MECA) from cloned hA_3 receptor stably expressed in Chinese hamster ovary (CHO) cells. Subsequently, we selected compounds **1**, **4**−**6**, **8**, **10**−**12**, **14**−**20**, which showed high A_3 AR affinity (K_i < 50 nM), and the previously reported **A** and **B** and tested them for their ability to displace [^{3}H]DPCPX from cloned hA_1 AR in order to establish their A_3 vs A_1 selectivity within the same species. Finally, compounds **A**, **B**, **1**, **4**−**6**, **8**, **10**−**12**, **14**−**20**, most of which were highly A_3 vs A_1 selective, were also tested for their ability to displace [^{3}H]-5′-(*N*-ethylcarboxamido)adenosine ([^{3}H]NECA) from cloned hA_{2A} ARs. The binding results of **1**−**23**, together with those of compounds **A** and **B** for comparison, are shown in Table 1. The binding data of theophylline and 1,3-dipropyl-8-cyclopentylxanthine (DPCPX), included as antagonist reference compounds, are also reported.

Compounds **11**, **12**, **19**, and **20**, which showed high hA_3 and null hA_1 and hA_{2A} AR affinities, were also tested at hA_{2B} AR. In particular, their inhibitory effects on NECA-stimulated cAMP levels in hA_{2B} CHO cells were measured. The same functional assay was performed on hA_3 CHO cells in order to assess the antagonistic potencies of **11**, **12**, **19**, and **20** at the hA_3 receptor subtype. The antagonism of these derivatives on 2-chloro-N^6-(3-iodobenzyl)-5′-(*N*-methylcarbamoyl)adenosine (Cl-IB-MECA) inhibited cAMP production was determined. The results of these functional studies are reported in Table 2 and Figure 1.

Table 2. Potency of Compounds **11**, **12**, **19**, and **20** versus hA_{2B} and hA_3 Adenosine Receptor Subtypes

	IC_{50} [a] (nM) of cAMP assays	
	for hA_{2B}CHO cells	for hA_3CHO cells
11	>1000 (17%)	8.6 ± 0.9
12	>1000 (37%)	215 ± 20
19	>1000 (15%)	28.3 ± 2.7
20	>1000 (13%)	31.8 ± 2.1

[a] The data are expressed as the mean ± SEM of four independent experiments performed in triplicate. In parentheses are indicated the percentages of inhibition at 1 μM compound of the cAMP levels, stimulated by the presence of 200 nM NECA for A_{2B} adenosine receptors or inhibited by 100 nM Cl-IB-MECA for A_3 adenosine receptors.

Results and Discussion

The binding results showed that the structural modifications carried out on the 4-amino-2-phenyl-1,2,4-triazolo[4,3-*a*]qui-

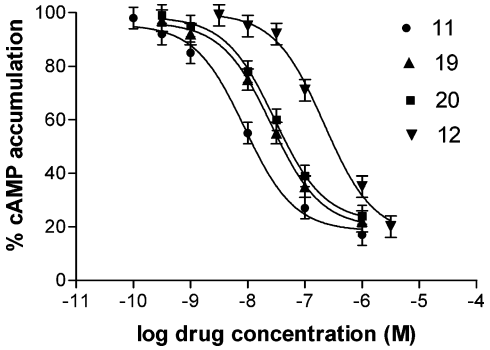

Figure 1. Inhibition curves of cAMP accumulation to human A_3 adenosine receptors expressed in CHO cells by examined antagonists.

noxalin-1-one framework have produced positive effects (Table 1). In fact, the novel derivatives **1**−**23** possess, on the whole, nanomolar hA_3 AR affinities and high selectivity versus this AR subtype. We have also obtained some potent (K_i < 50 nM) bA_1 AR antagonists (compounds **2**, **4**, **10**, **12**, **14**, **15**, **17**, **19**), while, as expected, the new derivatives are generally inactive at the bA_{2A} AR.

It should first be pointed out that the newly investigated 4-diphenylacetylamino and 4-dibenzoylamino moieties (derivatives **14** and **19**, respectively) elicited a profitable effect in terms of hA_3 AR affinity, similar to that previously exerted by the 4-acetylamino and 4-benzoylamino groups (derivatives **A** and **B**, respectively). Indeed, both compounds **14** and **19** bind to the hA_3 receptor with nanomolar affinities (K_i = 0.8 and 5.2 nM, respectively). The 4-dibenzoylamino compound **19** also displayed high selectivity, being completely inactive at both hA_1 and hA_{2A} AR. In contrast, the 4-diphenylacetylamino derivative **14** is only highly hA_3 vs hA_{2A} selective, since it maintains nanomolar affinity at the hA_1 AR.

Interesting results were also obtained when suitable substituents were introduced at the R_1 (OMe) and/or R_6 (NO_2, NH_2) positions of the parent compounds **A**, **B**, **14**, and **19.** The 4-benzoylamino derivatives **6** and **8**−**11**, the 4-diphenylacetylamino compounds **12** and **15**−**18**, and the 4-dibenzoylamino-substituted derivatives **20** and **22** possess, on the whole, better hA_3 AR affinities than the corresponding 4-acetylamino derivatives **1**−**5** probably because of the stronger lipophilic interactions that the benzoyl, diphenylacetyl, or dibenzoyl residues, with respect to the acetyl group, can engage in with the receptor site. Moreover, the greater steric hindrance of compounds **6**−**20** at the 4-position level suggests the existence of a roomy receptor pocket that can hold the 4-acylamino moiety of these derivatives.

Insertion of the R_1 = OMe on the 2-phenyl ring of all the 4-acylaminotriazoloquinoxalin-1-one derivatives (**A**, **B**, **14**, **19**) left the hA_3 AR affinity unchanged (compounds **6** and **20**) or slightly reduced (derivatives **1** and **12**) while, more importantly, it significantly increased hA_3 vs hA_1 selectivity. Interestingly, all the 2-(4-methoxyphenyl)-substituted derivatives were poorly active (**6**) or totally inactive (**1**, **12**, **20**) at the hA_{2A} receptor subtype. A dramatic reduction of hA_3 affinity was observed when the nitro substituent was placed at the R_1-position. Indeed, the 4-benzoylamino compound **7** and 4-diphenylacetylamino derivative **13** are significantly less active than the corresponding derivatives **B** and **14**, lacking the nitro group. In particular, compound **13** showed null affinity at all the investigated receptors. However, the negative effect of R_1 = NO_2 is consistent with our previous data.[21]

The presence of the 6-nitro substituent did not always produce advantageous effects. This modification was profitable on **B** and **14**, since it maintained high hA_3 affinity and significantly increased selectivity (compounds **8** and **15**); yet when performed on **A** and **19**, it dramatically dropped hA_3 AR affinities (compounds **2** and **21**). Instead, introduction of the 6-amino group turned out to be positive because, on the whole, it afforded active compounds that possess nanomolar hA_3 affinities (**4**, **10**, and **17**) and also (**4** and **10**) high hA_3 vs hA_1 selectivity. The contemporary presence of R_1 = OMe and R_6 = NO_2 generally decreased hA_3 AR affinity (compounds **3**, **9**, and **22**) with the only exception of the 2-diphenylacetamido derivative **16**, which is highly potent (K_i = 0.8 nM) and selective at the hA_3 AR. Interestingly, the double substitution with R_1 = OMe and R_6 = NH_2, present in compounds **5**, **11**, **18**, preserved the high hA_3 affinities (K_i = 1−5.5 nM) of the corresponding unsubstituted derivatives **A**, **B**, and **14** and also afforded high hA_3 AR selectivity.

Compounds **11**, **12**, **19**, and **20**, which showed high hA_3 and null hA_1 and hA_{2A} AR affinities, were also tested at the A_{2B} AR by evaluating their inhibitory effects on cAMP accumulation in CHO cells stably expressing the hA_{2B} AR (Table 2). These derivatives resulted in being inactive in this assay, thus indicating a complete lack of affinity toward the hA_{2B} AR. In contrast, **11**, **12**, **19**, and **20** were highly potent in the same assay performed on hA_3 CHO cells. The potencies of these derivatives in antagonizing the Cl-IB-MECA-inhibited cAMP production are in accordance with their hA_3 AR affinity values (Table 2 and Figure 1).

The bA_1 AR and bA_{2A} binding data (Table 1) warrant some comments. As expected, compounds **1**−**23** are inactive at the bA_{2A} receptor subtype, with the exception of three derivatives (**4**, **14**, and **20**), which possess bA_{2A} micromolar affinities. In contrast, only seven compounds (**3**, **7**−**9**, **13**, **21**, and **22**) are inactive at the bA_1 receptor while all the others show bA_1 AR affinities that span the nanomolar range.

A comparison of the bA_1 affinity values with the corresponding hA_1 AR ones confirms that species differences exist not only for the A_3 receptor but also for the A_1 subtype.[24−26] Indeed, previously reported data[21] and herein-reported data indicate that in this class of derivatives the hA_1 AR affinities are, overall, significantly lower than the bA_1 AR affinities. Only compounds **B**, **10**, and **14** show a similar nanomolar affinity at both receptor types. Structural differences also exist between the A_{2A} receptors of human and bovine species. In fact, some of the tested derivatives (**B**, **4**−**6**, **10**, **14**, **17**, **20**) showed quite different affinities at the two receptors, being in general more active at the hA_{2A} receptor (**B**, **4**−**6**, **10**, **17**).

The bA_1 binding data, in accordance with our previous finding,[17,21] point out the capability of the 4-methoxy group on the 2-phenyl ring to significantly decrease affinity. Indeed, derivatives **1**, **6**, and **20**, bearing this substituent, are less active at the bA_1 AR than the corresponding 2-phenyl derivatives **A**, **B**, and **19**, and only the 2-(4-methoxyphenyl)-4-diphenylacetylamino derivative **12** is equiactive to the des-methoxy compound **14**. Different from the para methoxy substituent, the 6-nitro group does not exert a constant effect on bA_1 affinity. Indeed, the 4-benzoylamino- and the 4-dibenzoylamino-substituted derivatives **8** and **21** are less active than the corresponding 6-des-nitro derivatives **B** and **19** while the 4-acetylamino derivative **2** and the 4-diphenylacetylamino compound **15** show nanomolar affinities comparable to those of their analogues **A** and **14**. The unpredictable effect of the 6-nitro group is consistent with our previous data obtained on this class of derivatives.[21] Introduction of the 6-amino residue (compounds **4**, **10**, **17**, **23**) left the bA_1 affinity almost unchanged, with the exception of compound **17** which is 10-fold more active than the corresponding 6-des-amino

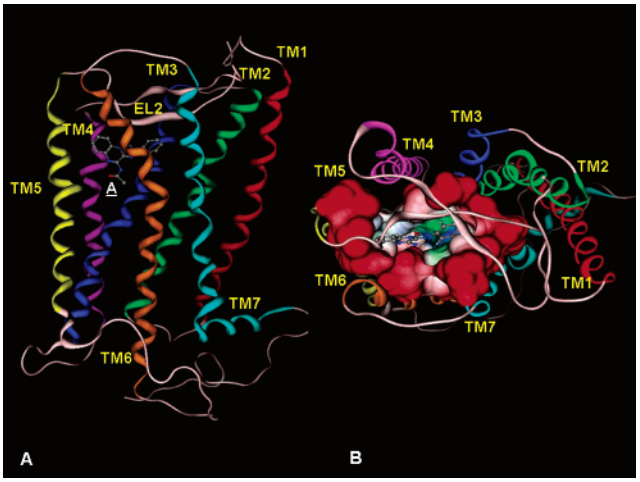

Figure 2. Human A_3 receptor model viewed from the membrane side (A) and from the extracellular side (B) showing the E2 loop folded into the binding crevice. Putative binding sites suggested by site-directed mutagenesis studies are delimited by the docked derivative **A**.

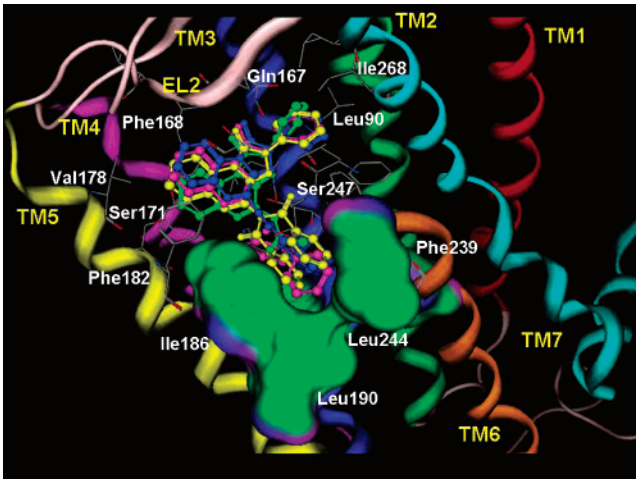

Figure 3. Hypothetical binding motif of the representative newly synthesized 4-amino-2-phenyl-1,2,4-triazolo[4,3-*a*]quinoxalin-1-one antagonists (derivative **A** in green, derivative **B** in blue, derivative **12** in magenta, and derivative **19** in yellow). All docked antagonists are viewed from the membrane side facing TM helices 5 and 6. To clarify the TM cavity, the view of TM6 from Pro245 to Phe255 has been voluntarily omitted. Side chains of some amino acids important for ligand recognition are highlighted. Hydrogen atoms are not displayed. Moreover, the receptor region around the R_4 substituents characterized by five nonpolar amino acids, Ile98 (TM3), Ile186 (TM5), Leu190 (TM5), Phe239 (TM6), and Leu244 (TM6), has been represented by its Connolly's molecular surface.

derivative **14**. Interestingly, the para methoxy group maintains its capability of decreasing the bA_1 AR affinity even when the 6-nitro (compounds **3**, **9**, **16**, **22**) or the 6-amino group (compounds **5**, **11**, **18**) is present on the triazoloquinoxaline nucleus. In fact, these 2-(4-methoxyphenyl) derivatives are, on the whole, significantly less active than the corresponding 2-phenyl substituted analogues.

Following our recently reported modeling investigations, we used our improved model of the hA_3 receptor, obtained by a rhodopsin-based homology modeling approach,[21−23,27−31] to recognize the hypothetical binding motif of these newly synthesized 4-amino-2-phenyl-1,2,4-triazolo[4,3-*a*]quinoxalin-1-one antagonists. From analysis of docking simulation results, all triazoloquinoxalinone derivatives share a similar binding motif inside the transmembrane (TM) region of the hA_3 receptor, as previously described.[21,27−31] As shown in Figure 2, we identified the hypothetical binding site of the triazoloquinoxalinone moiety surrounded by TMs 3, 5, 6, and 7 with the carbonyl group at 1-position pointing toward the EL2 and with the amide moiety in the 4-position oriented toward the intracellular environment. The phenyl ring at the 2-position is close to TMs 3, 6, and 7, whereas R_6 substituents are close to TM5. For a clear explanation of the observed structure−activity relationships, it is useful to immediately emphasize that the relative positions of the R_6 substituents are slightly different depending on the bulkiness of the R_4 substituent on the 4-amide moiety, as shown in Figure 3. However, the overall pharmacophore features are nicely consistent with our recently proposed receptor-based pharmacophore model.[29−31] From analysis of our model in detail, all triazoloquinoxalinone derivatives share at least two stabilizing hydrogen-bonding interactions inside the binding cleft. The first hydrogen bonding is between the carbonyl group at the 1-position, pointing toward the EL2, and the NH of the Gln167−Phe168 amidic bond. This hydrogen-bonding distance is calculated to be around 2.8 Å for all docked compounds. Moreover, the 1-carbonyl group is also at the hydrogen-bonding distance with the amide moiety of Asn250 (TM6) side chain. This asparagine residue, conserved among all adenosine receptor subtypes, was found to be important for ligand binding. Second, the NH−CO moiety at the 4-position is surrounded by three polar amino acids: Thr94 (TM3), His95 (TM3), and Ser247 (TM6). This region seems to be very critical for the recognition of all antagonist structures. In fact, a major structural difference between the hypothetical binding sites in these receptor subtypes is that the A_3 receptor does not contain the histidine residue in TM6 common to all A_1 (His251 in hA_1) and A_2 (His250 in hA_{2A}) receptors. This histidine has been shown to participate in both agonist and antagonist binding to A_{2A} receptors. In the A_3 receptor this histidine in TM6 is replaced by a serine residue (Ser247 in hA_3).[32] The stabilizing interactions among the 4-carbamoyl moiety and these polar amino acids orient the adjacent R_4 substituent (methyl, **A** and **1**−**5**; phenyl, **B** and **6**−**11**; diphenylmethyl, **12**−**18**) in the middle of the TM bundle. In particular, the O−H of Ser247 (TM6) and the carbonyl oxygen of the amide group are separated by 2.4 Å and appropriately oriented to form a H-bonding interaction. Moreover, the side chain of His95 (TM3) is within dipole−dipole interaction distance of NH of the amide group, at around 2.9 Å. According to recently published mutagenesis results, both His95 and Ser247 seem to affect the binding of both agonists and antagonists.[32] Indeed, the receptor region around R_4 substituents is mostly hydrophobic and characterized by five nonpolar amino acids: Ile98 (TM3), Ile186 (TM5), Leu190 (TM5), Phe239 (TM6), and Leu244 (TM6) (Figure 2).

Considering the observed structure−activity relationships in greater detail, methoxy substitution at the R_1-position is rather well tolerated among all newly synthesized triazoloquinoxalinone derivatives. This is consistent with its accommodation into a tiny hydrophobic pocket delimited by Leu90 (TM3) and Ile268 (TM7). Interestingly, the amino acid corresponding to Leu90 in the hA_{2A} receptor was found to be essential for the binding of both agonists and antagonists, and it is mutated in valine (Val87) in the human A_1 receptor. This mutation might play a role in the explanation of hA_3 versus hA_1 selectivity. In fact, even if the mutation Leu90 (hA_3)/Val87 (hA_1) can slightly enlarge the dimension of this hydrophobic cavity, at the same time it also notably decreases the shape and hydrophobic interaction complementarity (data not shown). Also, the mutation of Ser165 (EL2 of hA_3) with Lys168 in the hA_1 receptor could affect the recognition of the methoxy-substituted triazoloquinoxalinone derivatives. Considering the same small pocket

surrounded by Leu90 (TM3) and Ile268 (TM7), unfavorable steric and dipolar interactions are responsible for the reduction of affinity observed for derivatives **7** and **13**, whereas the methoxy substituent at R_1 is replaced by the nitro group.

On the other hand, the presence of the 6-nitro substituent does not always produce advantageous effects in terms of hA_3 AR binding affinity. This phenomenon is particularly evident when derivatives **2** and **15** are compared with their unsubstituted compounds **A** and **14**. As already anticipated and clearly shown in Figure 3, the relative positions of R_6 substituents are slightly different depending on the bulkiness of the R_4 substituent on the carbamoyl moiety at the 4-position. In particular, in the presence of a less bulky R_4 substituent such as a methyl group (derivative **A**), the triazoloquinoxalinone moiety binds more deeply in the middle of the TM bundle, positioning the 6-nitro substituent very close to TM5. In this case, unfavorable steric and dipolar interactions are responsible for the remarkable reduction of affinity observed for derivatives **2** and **3**. In contrast, the smaller 6-amino substituent (derivatives **4** and **5**) is still well tolerated because of the favorable dipolar interaction with the carbonyl moiety of the Ser181−Phe182 amidic bond. When the bulkiness of the R_4 substituent is increased, the position of the R_6 group shifts away from TM5, and consequently, more empty space is available for the 6-nitro substituent, such as in derivatives **8**, **15**, and **16**.

Considering the 4-dibenzoyl derivatives **19**−**23**, the simultaneous presence of two bulky substituents at the 4-position forces a slight rearrangement of the triazoloquinoxalinone moiety inside the TM binding cavity (Figure 3). Curiously, while the position of the methoxy substitution at the R_1-position is relatively well conserved compared with all other triazoloquinoxalinone derivatives, the R_6 substituents are much closer to the R_6 position of derivative **2** and consequently much closer to the TM5 domain. As already described for compound **2**, in this case the unfavorable steric and dipolar interactions are probably responsible for the remarkable reduction of affinity of derivatives **21** and **22**. To explain the different behavior of derivatives **21** ($R_6 = NO_2$; $I = 27\%$ at 1 μM) and **23** ($R_6 = NH_2$; $K_i \cong 1200$ nM), we can apply the same argument already used for the comparison of derivatives **2** and **4**.

Conclusion

The present study has led to the identification of new potent and selective hA_3 AR antagonists. As expected, most of the substitution patterns of the 1,2,4-triazolo[4,3-*a*]quinoxalin-1-one nucleus were effective in shifting affinity toward the hA_3 receptor. Most importantly, an integrated SAR and molecular docking study provided new interesting insights about the fine steric and electrostatic control that is involved in the anchoring of this class of compounds to the hA_3 receptor binding site.

The rationalization of all experimental SAR findings, using our recently proposed rhodopsin-based homology model of the human A_3 receptor, is further evidence supporting our belief that the reciprocal integration of different theoretical and experimental disciplines can be very useful for the successful design of new, potent, and selective GPCR ligands.

Experimental Section

(A) Chemistry. Silica gel plates (Merck F254) and silica gel 60 (Merck, 70−230 mesh) were used for analytical and column chromatography, respectively. All melting points were determined on a Gallenkamp melting point apparatus. Microanalyses were performed with a Perkin-Elmer 260 elemental analyzer for C, H, N, and the results were within ±0.4% of the theoretical values, unless otherwise stated. The IR spectra were recorded with a Perkin-Elmer Spectrum RX I spectrometer in Nujol mulls and are expressed in cm^{-1}. The ^1H NMR spectra were obtained with a Brucker Avance 400 MHz instrument. The chemical shifts are reported in δ (ppm) and are relative to the central peak of the solvent, which was always DMSO-d_6. The following abbreviations are used: s = singlet, d = doublet, dd = double doublet, t = triplet, m = multiplet, br = broad, and ar = aromatic protons.

Synthesis of 4-Acetamido-2-(4-methoxyphenyl)-1,2-dihydro-1,2,4-triazolo[4,3-*a*]quinoxalin-1-one (1). A solution of acetyl chloride (2.1 mmol) in anhydrous dichloromethane (5 mL) was added to a suspension of 4-amino-2-(4-methoxyphenyl)-1,2,4-triazolo[4,3-*a*]quinoxalin-1-one **C**[17] (0.7 mmol) in anhydrous dichloromethane (20 mL) and anhydrous pyridine (9.8 mmol, 0.7 mL). The mixture was stirred at room temperature for 12 h. Evaporation of the solvent at reduced pressure gave a residue that was treated with water/ethanol, collected by filtration, and washed with water. Yield, 92%; mp 276−278 °C (DMF/EtOH). ^1H NMR 2.33 (s, 3H, $COCH_3$), 3.81 (s, 3H, OCH_3), 7.12 (d, 2H, ar, $J = 9.1$ Hz), 7.42−7.61 (m, 2H, ar), 7.72 (d, 1H, ar, $J = 7.7$ Hz), 7.95 (d, 2H, ar, $J = 8.1$ Hz), 8.72 (d, 1H, H-9, $J = 7.7$ Hz), 10.57 (s, 1H, NH). IR 1690, 1730, 3200, 3220. Anal. ($C_{18}H_{15}N_5O_3$) C, H, N.

Synthesis of 4-Acetamido-1,2-dihydro-6-nitro-2-phenyl-1,2,4-triazolo[4,3-*a*]quinoxalin-1-one (2). A mixture of 4-amino-6-nitro-2-phenyl-1,2,4-triazolo[4,3-*a*]quinoxalin-1-one **D**[18] (0.6 mmol), acetic anhydride (1.8 mmol, 0.17 mL), 4-(dimethylamino)pyridine (0.07 mmol, 0.1 mg), and triethylamine (9 mmol, 1.2 mL) in anhydrous dimethylformamide (5 mL) was stirred at room temperature for 3 h. The solid was collected by filtration and washed with water and ethanol. Yield, 78%; mp >300 °C (CH_3NO_2). ^1H NMR 2.39 (s, 3H, CH_3), 7.36 (t, 1H, ar, $J = 8.1$ Hz), 7.51−7.75 (m, 3H, ar), 7.92 (d, 1H, ar, $J = 7.7$ Hz), 8.10 (d, 2H, ar, $J = 7.7$ Hz), 8.85 (d, 1H, H-9, $J = 8.1$ Hz), 10.83 (s, 1H, NH). IR 1650, 1730, 3300, 3360. Anal. ($C_{17}H_{12}N_6O_4$) C, H, N.

Synthesis of 4-Acetamido-1,2-dihydro-6-nitro-2-(4-methoxyphenyl)-1,2,4-triazolo[4,3-*a*]quinoxalin-1-one (3). Acetyl chloride (3.39 mmol) was added to a suspension of 4-amino-2-(4-methoxyphenyl)-6-nitro-1,2,4-triazolo[4,3-*a*]quinoxalin-1-one **E**[21] (1.13 mmol) in anhydrous pyridine (5 mL). The mixture was refluxed for 12 h and then diluted with water (10 mL). The solid was collected by filtration and washed with water. Yield, 89%; mp 292−294 °C (DMF). ^1H NMR 2.41 (s, 3H, CH_3), 3.83 (s, 3H, OMe), 7.15 (d, 2H, ar), 7.70 (t, 1H, ar, $J = 9.1$ Hz), 7.93−8.00 (m, 3H, ar), 8.88 (d, 1H, H-9, $J = 7.9$ Hz), 10.82 (s, 1H, NH). IR 1692, 1714, 3200. Anal. ($C_{18}H_{14}N_6O_5$) C, H, N.

General Procedure for the Synthesis of 4-Acetamido-6-amino-2-aryl-1,2-dihydro-1,2,4-triazolo[4,3-*a*]quinoxalin-1-ones (4 and 5). The 6-nitro derivative **2** or **3** (1.2 mmol) was dissolved in hot DMF (50 mL for **2** and 15 mL for **3**), and 10% Pd/C (10% w/w) was added to the solution. The mixture was hydrogenated in a Parr apparatus at 40 psi for 12 h. The catalyst was filtered off, and the clear solution was diluted with water (50 mL). The solid that precipitated was collected by suction and washed with water.

4: yield, 75%; mp 281−282 °C (DMF). ^1H NMR 2.35 (s, 3H, CH_3), 5.75 (s, 2H, NH_2), 6.77 (d, 1H, ar, $J = 8.0$ Hz), 7.24 (t, 1H, ar, $J = 8.0$ Hz), 7.37 (t, 1H, ar, $J = 7.3$ Hz), 7.57 (t, 2H, ar, $J = 8.2$ Hz), 7.87 (d, 1H, ar, $J = 8.0$ Hz), 8.09 (d, 2H, ar, $J = 8.2$ Hz), 10.41 (s, 1H, NH). IR 1679, 1701, 1714, 3186, 3234, 3359, 3478. Anal. ($C_{17}H_{14}N_6O_2$) C, H, N.

5: yield, 55%; mp 247−249 °C (2-methoxyethanol). ^1H NMR 2.34 (s, 3H, COMe), 3.82 (s, 3H, OMe), 5.74 (s, 2H, NH_2), 6.77 (d, 1H, ar, $J = 8.1$ Hz), 7.12 (d, 2H, ar, $J = 9.0$ Hz), 7.23 (t, 1H, ar, $J = 8.1$ Hz), 7.87 (d, 1H, ar, $J = 8.1$ Hz), 7.94 (d, 2H, ar, $J = 9.0$ Hz), 10.41 (s, 1H, NH). IR 1683, 1705, 3180, 3240, 3357. Anal. ($C_{18}H_{16}N_6O_3$) C, H, N.

General Procedure for the Synthesis of 4-Benzamido-2-(4-methoxyphenyl)-1,2-dihydro-1,2,4-triazolo[4,3-*a*]quinoxalin-1-one (6), 4-Benzamido-6-nitro-2-phenyl-1,2-dihydro-1,2,4-triazolo-[4,3-*a*]quinoxalin-1-one (8), and 4-Benzamido-2-(4-methoxyphenyl)-6-nitro-1,2-dihydro-1,2,4-triazolo[4,3-*a*]quinoxalin-1-one (9). Benzoyl chloride (2.1 mmol) was added to a suspension of derivative **C**,[17] **D**,[18] or **E**[21] (0.7 mmol) in anhydrous dichloromethane

(20 mL) and anhydrous pyridine (0.7 mL). The mixture was refluxed until the disappearance (TLC monitoring) of the starting material (6−20 h). Evaporation of the solvent at reduced pressure gave a residue, which was treated with water (5 mL) and a few drops of ethanol, collected by filtration, and washed with water.

6: yield, 40%; mp 203−205 °C (cyclohexane/ethyl acetate). ^{1}H NMR 3.80 (s, 3H, CH_3), 7.10 (d, 2H, ar, J = 9.2 Hz), 7.53−7.65 (m, 5H, ar), 7.78−7.86 (m, 3H, ar), 8.07 (d, 2H, ar, J = 7.7 Hz), 8.78 (d, 1H, H-9, J = 7.7 Hz), 11.35 (br s, 1H, NH). IR 1690, 1720, 3240. Anal. ($C_{23}H_{17}N_5O_3$) C, H, N.

8: yield, 80%; mp 290−292 °C (DMF). ^{1}H NMR 7.38 (d, 1H, ar, J = 7.9 Hz), 7.44−8.20 (m, 10H, ar), 8.26−8.30 (m, 1H, ar), 8.93 (d, 1H, H-9, J = 8.2 Hz), 11.43 (br s, 1H, NH). Anal. ($C_{22}H_{14}N_6O_4$) C, H, N.

9: yield, 68%; mp 278−280 °C (DMF). ^{1}H NMR 3.80 (s, 3H, OMe), 7.11 (d, 2H, ar, J = 8.4 Hz), 7.48−8.40 (m, 9H, ar), 8.90 (d, 1H, H-9, J = 8.0 Hz), 11.40 (br s, 1H, NH). Anal. ($C_{23}H_{16}N_6O_5$) C, H, N.

Synthesis of 4-Benzamido-1,2-dihydro-2-(4-nitrophenyl)-1,2,4-triazolo[4,3-*a*]quinoxalin-1-one (7). A mixture of 4-amino-2-(4-nitrophenyl)-1,2,4-triazolo[4,3-*a*]quinoxalin-1-one derivative **24**[21] (0.46 mmol) and benzoyl chloride (0.92 mmol) in anhydrous pyridine (10 mL) was refluxed for 48 h. After cooling at room temperature, the suspension was diluted with water (4 mL) and the solid was collected by filtration and washed with water. Yield, 85%; mp >300 °C (DMF). ^{1}H NMR 7.68 (m, 5H, ar), 7.79 (d, 1H, ar, J = 8.1 Hz), 8.01−8.07 (m, 2H, ar), 8.32 (d, 2H, ar, J = 9.5 Hz), 8.43 (d, 2H, ar, J = 9.5 Hz), 8.73 (d, 1H, H-9, J = 8.1 Hz), 11.28 (br s, 1H, NH). IR 1360, 1553, 1672, 1726, 3115, 3211. Anal. ($C_{22}H_{14}N_6O_4$) C, H, N.

General Procedure for the Synthesis of 6-Amino-4-benzamido-1,2-dihydro-2-phenyl-1,2,4-triazolo[4,3-*a*]quinoxalin-1-one (10) and 6-Amino-4-benzamido-1,2-dihydro-2-(4-methoxyphenyl)-1,2,4-triazolo[4,3-*a*]quinoxalin-1-one (11). The 10% Pd/C (0.03 g) was added to a solution of the 6-nitro derivative **8** or **9** (0.7 mmol) in dimethylformamide (50 mL). The mixture was hydrogenated in a Parr apparatus at 30 psi for 3 h, the catalyst was filtered off, and the clear solution was diluted with water. The solid that precipitated was collected by filtration and washed with water and ethanol.

10: yield, 85%; mp 235−237 °C (2-methoxyethanol). ^{1}H NMR 5.82 (s, 2H, NH_2), 6.78 (d, 1H, ar, J = 8.4 Hz), 7.26−7.66 (m, 7H, ar), 7.89−8.05 (m, 5H, ar), 11.02 (br s, 1H, NH). IR 1668, 1727, 3312, 3359, 3456. Anal. ($C_{22}H_{16}N_6O_2$) C, H, N.

11: yield, 90%; mp 264−266 °C (DMF). ^{1}H NMR 3.77 (s, 3H, CH_3), 5.81 (s, 2H, NH_2), 6.77 (d, 1H, ar, J = 8.1 Hz), 7.06 (d, 2H, ar, J = 9.2 Hz), 7.28 (t, 1H, ar, J = 8.1 Hz), 7.51−7.69 (m, 3H, ar), 7.80−8.04 (m, 5H, ar), 10.98 (s, 1H, NH). IR 1681, 1720, 3290, 3352, 3445. Anal. ($C_{23}H_{18}N_6O_3$) C, H, N.

General Procedure for the Synthesis of 2-Aryl-1,2-dihydro-4-diphenylacetamido-1,2,4-triazolo[4,3-*a*]quinoxalin-1-ones (12−14) and 2-Aryl-1,2-dihydro-6-nitro-4-diphenylacetamido-1,2,4-triazolo[4,3-*a*]quinoxalin-1-ones (15 and 16). The 4-amino-1,2,4-triazolo[4,3-*a*]quinoxalin-1-one derivatives **C**,[17] **24**,[21] **25**,[17] **D**,[18] and **E**[21] (0.46 mmol) were reacted with diphenylacetyl chloride (0.92 mmol) in refluxing anhydrous pyridine (10 mL) until the disappearance (TLC monitoring) of the starting material (10−12 h). After cooling at room temperature, the mixture was diluted with water (20 mL) and the solid was collected by filtration and washed with water.

12: yield, 65%; mp 251−252 °C (DMF). ^{1}H NMR 3.83 (s, 3H, CH_3), 5.73 (s, 1H, CH), 7.15 (d, 2H, ar, J = 9.2 Hz), 7.21−7.80 (m, 13 H, ar), 7.92 (d, 2H, ar, J = 9.2 Hz), 8.76 (d, 1H, H-9, J = 7.5 Hz), 11.20 (br s, 1H, NH). Anal. ($C_{30}H_{23}N_5O_3$) C, H, N.

13: yield, 95%; mp 298−300 °C (DMF). ^{1}H NMR 5.76 (s, 1H, CH), 7.30−7.32 (m, 2H, ar), 7.38−7.45 (m, 8H, ar), 7.54 (t, 1H, ar, J = 7.9 Hz), 7.61 (t, 1H, ar, J = 7.8 Hz), 7.76 (d, 1H, ar, J = 6.8 Hz), 8.37 (d, 2H, ar, J = 8.5 Hz), 8.50 (d, 2H, ar, J = 8.5 Hz), 8.69 (d, 1H, H-9, J = 7.8 Hz), 11.16 (br s, 1H, NH). IR 1681, 1725, 3233. Anal. ($C_{29}H_{20}N_6O_4$) C, H, N.

14: yield, 55%; mp 226−227 °C (CH_3CN). ^{1}H NMR 5.68 (s, 1H, CH), 7.24−7.78 (m, 16H, ar), 8.05 (d, 2H, ar, J = 7.7 Hz), 8.75 (d, 1H, H-9, J = 7.3 Hz), 11.25 (br s, 1H, NH). Anal. ($C_{29}H_{21}N_5O_2$) C, H, N.

15: yield, 50%; mp >300 °C (2-methoxyethanol). ^{1}H NMR 6.00 (s, 1H, CH), 7.21−7.98 (m, 14H, ar), 7.96 (d, 1H, ar, J = 7.0 Hz), 8.08 (d, 2H, ar, J = 7.7 Hz), 8.89 (d, 1H, H-9, J = 7.8 Hz), 11.30 (br s, 1H, NH). IR 1374, 1555, 1691, 1729, 3183, 3233. Anal. ($C_{29}H_{20}N_6O_4$) C, H, N.

16: yield, 98%; mp 234−236 °C (DMF). ^{1}H NMR 3.83 (s, 3H, OMe), 5.96 (s, 1H, CH), 7.16 (d, 2H, ar, J = 9.1 Hz), 7.26−7.30 (m, 2H, ar), 7.31−7.40 (m, 8H, ar), 7.72 (t, 1H, ar, J = 8.2 Hz), 7.92−7.95 (m, 3H, ar), 8.87 (d, 1H, H-9), 11.23 (s, 1H, NH). IR 1689, 1719, 3226. Anal. ($C_{30}H_{22}N_6O_5$) C, H, N.

Synthesis of 6-Amino-1,2-dihydro-2-phenyl-4-diphenylacetamido-1,2,4-triazolo[4,3-*a*]quinoxalin-1-one (17). The title compound was obtained by catalytic hydrogenation of derivative **15** (1.2 mmol), dissolved in hot DMF (30 mL), following the procedure described above to prepare compounds **4** and **5**. Yield, 72%; mp 253−254 °C (2-methoxyethanol). ^{1}H NMR 5.65 (s, 1H, CH), 5.76 (s, 2H, NH_2), 6.76 (d, 1H, ar, J = 8.1 Hz), 7.24−7.31 (m, 3H, ar), 7.35−7.44 (m, 9H, ar), 7.58 (t, 2H, ar, J = 7.9 Hz), 7.87 (d, 1H, H-9, J = 8.0 Hz), 8.04 (d, 2H, ar, J = 7.8 Hz), 10.98 (br s, 1H, NH). IR 1693, 1708, 3257, 3364, 3473. Anal. ($C_{29}H_{22}N_6O_2$) C, H, N.

Synthesis of 6-Amino-1,2-dihydro-2-(methoxyphenyl)-4-diphenylacetamido-1,2,4-triazolo[4,3-*a*]quinoxalin-1-one (18). The 6-nitro derivative **16** (1.2 mmol) was dissolved in boiling ethyl acetate (100 mL), and 10% Pd/C (0.06 g) was added to the solution. The mixture was hydrogenated in a Parr apparatus at 30 psi for 12 h. The catalyst was filtered off, and the solvent was evaporated at reduced pressure. The solid residue was taken up with diethyl ether (10 mL) and collected by filtration. Yield, 65%; mp 230−232 °C (CH_3CN). ^{1}H NMR 3.83 (s, 3H, OMe), 5.64 (s, 1H, CH), 5.74 (s, 2H, NH_2), 6.76 (d, 1H, ar, J = 8.2 Hz), 7.14 (d, 2H, ar, J = 7.0 Hz), 7.23−7.30 (m, 3H, ar), 7.35−7.43 (m, 8H, ar), 7.86 (d, 1H, ar, J = 8.1 Hz), 7.91 (d, 2H, ar, J = 6.9 Hz), 10.95 (s, 1H, NH). IR 1693, 1708, 3257, 3364, 3473. Anal. ($C_{30}H_{24}N_6O_3$) C, H, N.

General Procedure for the Synthesis of 2-Aryl-4-dibenzamido-1,2-dihydro-1,2,4-triazolo[4,3-*a*]quinoxalin-1-ones (19 and 20) and 2-Aryl-4-dibenzamido-1,2-dihydro-6-nitro-1,2,4-triazolo[4,3-*a*]quinoxalin-1-ones (21 and 22). A mixture of **25**[17] or **C**[17] or **D**[18] or **E**[21] (1.2 mmol) and benzoyl chloride (12, 22.8, 7.2, or 36 mmol, respectively) in anhydrous pyridine (8 mL) was refluxed until the disappearance (TLC monitoring) of the starting material (18−20 h). After cooling at room temperature, the mixture was diluted with water (15 mL). The solid was collected by filtration and washed with water and diethyl ether.

19: yield, 74%; mp 236−238 °C (2-methoxyethanol). ^{1}H NMR 7.36 (t, 1H, ar, J = 7.4 Hz), 7.49−7.55 (m, 7H, ar), 7.62−7.71 (m, 3H, ar), 7.73 (t, 1H, ar, J = 7.1 Hz), 7.89−7.92 (m, 6H, ar), 8.77 (d, 1H, H-9, J = 7.4 Hz). IR 1703, 1730. Anal. ($C_{29}H_{19}N_5O_3$) C, H, N.

20: yield, 65%; mp 237−239 °C (2-methoxyethanol). ^{1}H NMR 3.79 (s, 3H, OMe), 7.09 (d, 2H, ar, J = 9.1 Hz), 7.50−7.53 (m, 5H, ar), 7.62−7.66 (m, 3H, ar), 7.71 (t, 1H, ar, J = 8.3 Hz), 7.78 (d, 2H, ar, J = 9.1 Hz), 7.90 (d, 4H, ar, J = 7.3 Hz), 8.77 (d, 1H, H-9, J = 8.3 Hz). IR 1707, 1729. Anal. ($C_{30}H_{21}N_5O_4$) C, H, N.

21: yield, 93%; mp 274−275 °C (2-methoxyethanol). ^{1}H NMR 7.37 (t, 1H, ar, J = 7.4 Hz), 7.53 (t, 6H, ar, J = 7.8 Hz), 7.67 (t, 2H, ar, J = 7.4 Hz), 7.85−7.94 (m, 8H, ar), 8.94 (d, 1H, H-9, J = 8.2 Hz). IR 1706, 1727. Anal. ($C_{29}H_{18}N_6O_5$) C, H, N.

22: yield, 60%; mp 280−281 °C (DMF). ^{1}H NMR 3.79 (s, 3H, OMe), 7.09 (d, 2H, ar, J = 9.1 Hz), 7.53 (t, 4H, ar, J = 7.7 Hz), 7.67 (t, 2H, ar, J = 7.4 Hz), 7.74 (d, 2H, ar, J = 9.1 Hz), 7.83−7.93 (m, 6H, ar), 8.93 (d, 1H, H-9, J = 8.2 Hz). IR 1687, 1715. Anal. ($C_{30}H_{20}N_6O_6$) C, H, N.

General Procedure for the Synthesis of 6-Amino-2-aryl-4-dibenzamido-1,2-dihydro-1,2,4-triazolo[4,3-*a*]quinoxalin-1-ones (23). Compound **23** was prepared by catalytic hydrogenation of the corresponding 6-nitro derivative **21** (1.2 mmol) dissolved in

boiling ethyl acetate (200 mL). The experimental procedure was the same as that described above to obtain derivative **18**. Crude derivative **23**, before recrystallization, was purified by column chromatography (SiO_2, eluting system cyclohexane/ethyl acetate 5.5/4.5). Yield, 78%; mp >300 °C (EtOH). ^{1}H NMR 5.83 (s, 2H, NH_2), 6.79 (d, 1H, ar, J = 8.2 Hz), 7.51 (m, 6H, ar, J = 7.4 Hz), 7.62 (t, 2H, ar, J = 7.4 Hz), 7.83 (d, 1H, ar, J = 8.0 Hz), 7.90 (d, 6H, ar, J = 7.1 Hz). IR 1700, 1723, 3374. Anal. ($C_{29}H_{20}N_6O_3$) C, H, N.

(B) Biochemistry. Bovine A_1 and A_{2A} Receptor Binding. Displacement of [^{3}H]CHA from A_1 ARs in bovine cerebral cortical membranes and [^{3}H]CGS 21680 from A_{2A} ARs in bovine striatal membranes was performed as described in ref 33.

Human A_1, A_{2A}, and A_3 Receptor Binding. Binding experiments at hA_1 and hA_3 ARs, stably expressed in CHO cells, were performed as previously described,[18] using [^{3}H]CHA and [^{125}I]AB-MECA, respectively, as radioligands. Displacement of [^{3}H]NECA from hA_{2A} ARs, stably expressed in CHO cells, was performed as reported in ref 25.

Measurement of Cyclic AMP Levels on CHO Cells Transfected with Human A_{2B} or A_3 Adenosine Receptors. CHO cells transfected with the human A_{2B} or A_3 adenosine receptors were suspended in 0.5 mL of incubation mixture containing 150 mM NaCl, 2.7 mM KCl, 0.37 mM NaH_2PO_4, 1 mM $MgSO_4$, 1 mM $CaCl_2$, 5 mM glucose, 5 mM Hepes, and 10 mM $MgCl_2$, pH 7.4, at 37 °C. Then 2.0 IU of adenosine deaminase/mL and 0.5 mM Ro 20-1724 as phosphodiesterase inhibitor were added and preincubated for 10 min in a shaking bath at 37 °C. A stock 10 mM solution of the tested compound was prepared in DMSO, and subsequent dilutions were accomplished in buffer. The effect of the examined compounds at different concentrations (0.1 nM to 1 μM) in the presence of Cl-IB-MECA (100 nM) for A_3 receptors or of NECA (200 nM) for A_{2B} receptors was evaluated for 10 min at 37 °C. The reaction was terminated by the addition of cold 6% trichloroacetic acid (TCA). The TCA suspension was centrifuged at 2000*g* for 10 min at 4 °C, and the supernatant was extracted four times with water-saturated diethyl ether. The final aqueous solution was tested for cAMP levels by a competition protein binding assay carried out according to the method of Varani et al.[34] Samples of cAMP standards (0−10 pmol) were added to each test tube containing 0.1 M trizma base, 8.0 mM aminophylline, 6.0 mM mercaptoethanol, pH 7.4, and [^{3}H]cAMP in a total volume of 0.5 mL. The binding protein, previously prepared from beef adrenals, was added to the samples and incubated at 4 °C for 150 min. At the end of the incubation time and after the addition of charcoal, the samples were centrifuged at 2000*g* for 10 min. The clear supernatant was mixed with 4 mL of Atomlight and counted in a LS-1800 Beckman scintillation counter.

Data Analysis. The concentration of the tested compounds that produced 50% inhibition of specific [^{3}H]CHA, [^{3}H]CGS 21680, or [^{125}I]AB-MECA binding (IC_{50}) was calculated using a nonlinear regression method implemented in the InPlot program (Graph-Pad, San Diego, CA) with five concentrations of displacer, each performed in triplicate. Inhibition constants (K_i) were calculated according to the Cheng−Prusoff equation.[35] The dissociation constants (K_d) of [^{3}H]CHA and [^{3}H]CGS 21680 in cortical and striatal bovine brain membranes were 1.2 and 14 nM, respectively. The K_d values of [^{3}H]CHA, [^{3}H]NECA, and [^{125}I]AB-MECA in hA_1, hA_{2A}, and hA_3 ARs in CHO cell membranes were 1.9, 30, and 1.4 nM, respectively.

EC_{50} and IC_{50} values obtained in cAMP assay were calculated by nonlinear regression analysis using the equation for a sigmoid concentration−response curve (Graph-PAD Prism, San Diego, CA).

(C) Computational Methodologies. All modeling studies were carried out on a 10 CPU (PIV-3.0GHZ and AMD64) Linux cluster running under openMosix architecture.[36] Homology modeling, energy calculation, and docking studies were performed using the Molecular Operating Environment (MOE, version 2005.06) suite.[37]

All docked structures were fully optimized without geometry constraints using RHF/AM1 semiempirical calculations. Vibrational frequency analysis was used to characterize the minima stationary points (zero imaginary frequencies). The software package MOPAC (version 7),[38] implemented in MOE suite, was utilized for all quantum mechanical calculations.

Homology Model of the hA_3 AR. On the basis of the assumption that GPCRs share similar TM boundaries and overall topology, a homology model of the hA_3 receptor was constructed. First, the amino acid sequences of TM helices of the A_3 receptor were aligned with those of bovine rhodopsin, guided by the highly conserved amino acid residues, including the DRY motif (D3.49, R3.50, and Y3.51) and three proline residues (P4.60, P6.50, and P7.50) in the TM segments of GPCRs. The same boundaries were applied to the TM helices of the A_3 receptor as they were identified from the X-ray crystal structure for the corresponding sequences of bovine rhodopsin,[39] the C_R coordinates of which were used to construct the seven TM helices for the hA_3 receptor. The loop domains of the hA_3 receptor were constructed by the loop search method implemented in MOE. In particular, loops are modeled first in random order. For each loop, a contact energy function analyzes the list of candidates collected in the segment searching stage, taking into account all atoms already modeled and any atoms specified by the user as belonging to the model environment. These energies are then used to make a Boltzmann-weighted choice from the candidates, the coordinates of which are then copied to the model. Any missing side chain atoms are modeled using the same procedure. Side chains belonging to residues whose backbone coordinates were copied from a template are modeled first, followed by side chains of modeled loops. Outgaps and their side chains are modeled last. Special caution has to be given to the second extracellular (E2) loop, which has been described in bovine rhodopsin as folding back over transmembrane helices[39] and, therefore, limiting the size of the active site. Hence, amino acids of this loop could be involved in direct interactions with the ligands. A driving force for this peculiar fold of the E2 loop might be the presence of a disulfide bridge between cysteines in TM3 and E2. Since this covalent link is conserved in all receptors modeled in the current study, the E2 loop was modeled using a rhodopsin-like constrained geometry around the E2−TM3 disulfide bridge. After the heavy atoms were modeled, all hydrogen atoms were added, and the protein coordinates were then minimized with MOE using the AMBER94 force field.[40] The minimizations were carried out by 1000 steps of steepest descent followed by conjugate gradient minimization until the rms gradient of the potential energy was less than 0.1 kcal mol^{-1} Å^{-1}. Protein stereochemistry evaluation was performed by several tools (Ramachandran and χ plots measure φ/ψ and χ_1/χ_2 angles and clash contacts reports) implemented in the MOE suite.[37]

Molecular Docking of the hA_3 AR Antagonists. All antagonist structures were docked into the hypothetical TM binding site by using the MOE-Dock tool, part of the MOE suite. Searching is conducted within a user-specified 3D docking box, using the Tabù Search protocol[41] and the MMFF94 force field.[42] MOE-Dock performs a user-specified number of independent docking runs (50 in our specific case) and writes the resulting conformations and their energies in a molecular database file. The resulting docked complexes were subjected to MMFF94 energy minimization until the rms of the conjugate gradient was <0.1 kcal mol^{-1} Å^{-1}. Charges for the ligands were imported from the MOPAC output files. To better refine all antagonist−receptor complexes, a rotamer exploration of all side chains involved in the antagonist binding was carried out. Rotamer exploration methodology was implemented in the MOE suite.[37]

Prediction of antagonist−receptor complex stability (in terms of the corresponding pK_i value) and the quantitative analysis for nonbonded intermolecular interactions (H-bonds, transition metal, water bridges, hydrophobic) were performed and visualized using several tools implemented in MOE suite.[37]

Acknowledgment. This work was supported by a grant from the Italian Ministry for University and Research (MIUR, FIRB RBNE03YA3L Project). The molecular modeling work coordinated by S.M. has been carried out with financial support from

the University of Padova, Italy, and the Italian Ministry for University and Research (MIUR), Rome, Italy. We thank Dr. Karl-Norbert Klotz of the University of Wüzburg, Germany, for providing cloned hA_1, hA_{2A}, and hA_3 receptors expressed in CHO cells. S.M. is also very grateful to Chemical Computing Group for the scientific and technical partnership.

Supporting Information Available: Combustion analysis data of the newly synthesized compounds. This material is available free of charge via the Internet at http://pubs.acs.org.

References

(1) Jacobson, K. A.; Knutsen, L. J. S. P1 and P2 purine and pyrimidine receptor ligands. In *Purinergic and Pyrimidinergic Signalling*; Abbracchio, M. P., Williams, M., Eds; Handbook of Experimental Pharmacology, Vol. 151/1; Berlin, Germany, 2001; pp 129−175.

(2) Jacobson, K. A.; Gao, Z. G. Adenosine receptors as therapeutic targets. *Nat. Rev. Drug Discovery* **2006**, *5*, 247−264.

(3) Linden, J.; Taylor, H. E.; Robeva, A. S.; Tucker, A. L.; Stehle, J. H.; Rivkees, S. A.; Fink, J. S.; Reppert, S. M. Molecular-cloning and functional expression of sheep A_3 adenosine receptor with widespread tissue distribution. *Mol. Pharmacol.* **1993**, *44*, 524−532.

(4) Abbracchio, M. P.; Brambilla, R.; Kim, H. O.; von Lubitz, D. K. J. E.; Jacobson, K. A.; Cattabeni, F. G-protein-dependent activation of phospholipase-C by adenosine A_3 receptor in rat brain. *Mol. Pharmacol.* **1995**, *48*, 1038−1045.

(5) Ali, H.; Choi, O. H.; Fraundorfer, P. F.; Yamada, K.; Gonzaga, H. M. S.; Beaven, M. A. Sustained activation of phospholipase-D via adenosine A_3 receptors is associated with enhancement of antigen-ionophore-induced and Ca^{2+}-ionophore-induced secretion in a rat mast-cell line. *J. Pharmacol. Exp. Ther.* **1996**, *276*, 837−845.

(6) Linden, J. Cloned adenosine A_3 receptors: pharmacological properties, species differences and receptor functions. *Trends Pharmacol. Sci.* **1994**, *15*, 298−306.

(7) Liang, B. T.; Jacobson, K. A. A physiological role of the adenosine A_3 receptor: sustained cardioprotection. *Proc. Natl. Acad. Sci. U.S.A.* **1998**, *95*, 6995−6999.

(8) Marx, D.; Ezeamuzie, C. I.; Nieber, K.; Szelenyi, I. Therapy of bronchial asthma with adenosine receptor agonists or antagonists. *Drug News Perspect.* **2001**, *14*, 89−100.

(9) Young, H. W.; Molina, J. G.; Dimina, D.; Zhong, H.; Jacobson, M.; Chan, L. N.; Chan, L.-N. L.; Chan, T.-S.; Lee, J. J.; Blackburn, M. R. A_3 adenosine receptor signaling contributes in airway inflammation and mucus production in adenosine deaminase-deficient mice. *J. Immunol.* **2004**, *173*, 1380−1389.

(10) Gessi, S.; Cattabriga, E.; Avitabile, A.; Gafâ, R.; Lanza, G.; Cavazzini, L.; Bianchi, N.; Gambari, R.; Feo, C.; Liboni, A.; Rullini, S.; Leung, E.; Mac-Lennan, S.; Borea, P. A. Elevated expression of A_3 adenosine receptors in human colorectal cancer is reflected in peripheral blood cells. *Clin. Cancer Res.* **2004**, *10*, 5895−5901.

(11) Merighi, S.; Mirandola, P.; Varani, K.; Gessi, S.; Leung, E.; Baraldi, P. G.; Tabrizi, M. A.; Borea, P. A. A glance at adenosine receptors: a novel target for antitumor therapy. *Pharmacol. Ther.* **2003**, *100*, 31−48.

(12) Brambilla, R.; Cattabeni, F.; Ceruti, S.; Barbieri, D.; Franceschi, C.; Kim, Y.-C.; Jacobson, K. A.; Klotz, K.-N.; Lohse, M. J.; Abbracchio, M. P.; Activation of the A_3 adenosine receptor affects cell cycle progression and cell growth. *Naunyn-Schmiedeberg's Arch. Pharmacol.* **2000**, *361*, 225−234.

(13) Pugliese, A. M.; Coppi, E.; Spalluto, G.; Corradetti, R.; Pedata, F. A_3 adenosine receptor antagonists delay irreversible synaptic failure caused by oxygen and glucose deprivation in the rat CA1 hippocampus in vitro. *Br. J. Pharmacol.* **2006**, *147*, 524−532.

(14) Catarzi, D.; Cecchi, L.; Colotta, V.; Filacchioni, G.; Martini, C.; Tacchi, P.; Lucacchini, A. Tricyclic heteroaromatic systems. Synthesis and A_1 and A_{2a} adenosine binding activities of some 1-aryl-1,4-dihydro-3-methyl[1]benzopyrano[2,3-*c*]pyrazol-4-ones, 1-aryl-4,9-dihydro-3-methyl-1*H*-pyrazolo[3,4-*b*]quinolin-4-ones, and 1-aryl-1*H*-imidazo[4,5-*b*]quinoxalines. *J. Med. Chem.* **1995**, *38*, 1330−1336.

(15) Colotta, V.; Catarzi, D.; Varano, F.; Cecchi, L.; Filacchioni, G.; Martini, C.; Trincavelli, L.; Lucacchini, A. 4-Amino-6-benzylamino-1,2-dihydro-2-phenyl-1,2,4-triazolo[4,3*a*]quinoxalin-1-one: a new A_{2A} adenosine receptor antagonist with high selectivity versus A_1 receptors. *Arch. Pharm. (Weinheim, Ger.)* **1999**, *332*, 39−41.

(16) Colotta, V.; Catarzi, D.; Varano, F.; Cecchi, L.; Filacchioni, G.; Martini, C.; Trincavelli, L.; Lucacchini, A. Synthesis and structure−activity relationships of a new set of 2-arylpyrazolo[3,4-*c*]quinoline derivatives as adenosine receptor antagonists. *J. Med. Chem.* **2000**, *43*, 3118−3124.

(17) Colotta, V.; Catarzi, D.; Varano, F.; Cecchi, L.; Filacchioni, G.; Martini, C.; Trincavelli, L.; Lucacchini, A. 1,2,4-Triazolo[4,3-*a*]-quinoxalin-1-one: a versatile tool for the synthesis of potent and selective adenosine receptor antagonists. *J. Med. Chem.* **2000**, *43*, 1158−1164.

(18) Colotta, V.; Catarzi, D.; Varano, F.; Filacchioni, G.; Martini, C.; Trincavelli, L.; Lucacchini, A. Synthesis and structure−activity relationships of a new set of 1,2,4-triazolo[4,3-*a*]quinoxalin-1-one derivatives as adenosine receptor antagonists. *Bioorg. Med. Chem.* **2003**, *11*, 3541−3550.

(19) Colotta, V.; Catarzi, D.; Varano, F.; Filacchioni, G.; Martini, C.; Trincavelli, L.; Lucacchini, A. Synthesis of 4-amino-6-(hetero)-arylalkylamino-1,2,4-triazolo[4,3-*a*]quinoxalin-1-one derivatives as potent A_{2A} adenosine receptor antagonists. *Bioorg. Med. Chem.* **2003**, *11*, 5509−5518.

(20) Colotta, V.; Catarzi, D.; Varano, F.; Filacchioni, G.; Martini, C.; Trincavelli, L.; Lucacchini, A. Synthesis and structure−activity relationships of 4-cycloalkylamino-1,2,4-triazolo[4,3-*a*]quinoxalin-1-one derivatives as A_1 and A_3 adenosine receptor antagonists. *Arch. Pharm. (Weinheim, Ger.)* **2004**, *337*, 35−41.

(21) Colotta, V.; Catarzi, D.; Varano, F.; Calabri, F. R.; Lenzi, O.; Filacchioni, G.; Trincavelli, L.; Martini, C.; Deflorian, F.; Moro, S. 1,2,4-Triazolo[4,3-*a*]quinoxalin-1-one moiety as an attractive scaffold to develop new potent and selective human A_3 adenosine receptor antagonists: synthesis, pharmacological and ligand−receptor modeling studies. *J. Med. Chem.* **2004**, *47*, 3580−3590.

(22) Catarzi, D.; Colotta, V.; Varano, F.; Calabri, F. R.; Lenzi, O.; Filacchioni, G.; Trincavelli, L.; Martini, C.; Tralli, A.; Montopoli, C.; Moro, S. 2-Aryl-8-chloro-1,2,4-triazolo[1,5-*a*]quinoxalin-4-amines as highly potent A_1 and A_3 adenosine receptor antagonists. *Bioorg. Med. Chem.* **2005**, *13*, 705−715.

(23) Catarzi, D.; Colotta, V.; Varano, F.; Lenzi, O.; Filacchioni, G.; Trincavelli, L.; Martini, C.; Montopoli, C.; Moro S. 1,2,4-Triazolo-[1,5-*a*]quinoxaline as a versatile tool for the design of selective human A_3 adenosine receptor antagonists: synthesis, biological evaluation and molecular modeling studies of 2-(hetero)aryl- and 2-carboxy-substituted derivatives. *J. Med. Chem.* **2005**, *48*, 7932−7945.

(24) Gao, Z.-G.; Blaustein, J. B.; Gross, A. S.; Melman, N.; Jacobson, K. A. N6-Substituted adenosine derivatives: selectivity, efficacy and species differences at A_3 adenosine receptors. *Biochem. Pharmacol.* **2003**, *65*, 1675−1684.

(25) Klotz, K.-N.; Hessling, J.; Hegler, J.; Owman, C.; Kull, B.; Fredholm, B. B.; Lohes, M. J. Comparative pharmacology of human adenosine receptor subtypes-characterization of stably transfected receptors in CHO cells. *Naunyn-Schiedeberg's Arch. Pharmacol.* **1998**, *357*, 1−9.

(26) Moro, S.; Gao, Z. G.; Jacobson, K. A.; Spalluto, G. Progress in the pursuit of therapeutic adenosine receptor antagonists. *Med. Res. Rev.* **2006**, *26*, 131−159.

(27) Moro, S.; Deflorian, F.; Spalluto, G.; Pastorin, G.; Cacciari, B.; et al. Demystifying the three dimensional structure of G protein-coupled receptors (GPCRs) with the aid of molecular modeling. *Chem. Commun. (Cambridge)* **2003**, *24*, 2949−2956.

(28) Moro, S.; Spalluto, G.; Jacobson, K. A. Techniques: Recent developments in computer-aided engineering of GPCR ligands using the human A_3 adenosine receptor as an example. *Trends Pharmacol. Sci.* **2005**, *26*, 44−51.

(29) Moro, S.; Braiuca, P.; Deflorian, F.; Ferrari, C.; Pastorin, G.; Cacciari, B.; Baraldi, P. G.; Varani, K.; Borea, P. A.; Spalluto, G. Combined target-based and ligand-based drug design approach as tool to define a novel 3D-pharmacophore model of human A_3 adenosine receptor antagonists: Pyrazolo[4, 3-*e*]1,2,4-triazolo[1, 5-*c*]pyrimidine derivatives as a key study. *J. Med. Chem.* **2005**, *48*, 152−162.

(30) Moro, S.; Deflorian, F.; Bacilieri, M.; Spalluto, G. Novel strategies for the design of new potent and selective human A_3 receptor antagonists: an update. *Curr. Med. Chem.* **2006**, *13*, 639−645.

(31) Moro, S.; Bacilieri, M.; Deflorian, F.; Spalluto, G. G protein-coupled receptors as challenging druggable targets: insights from *in silico* studies. *New J. Chem.* **2006**, *30*, 301−308.

(32) Gao, Z. G.; Chen, A.; Barak, D.; Kim, S. K.; Muller, C. E.; et al. Identification by site-directed mutagenesis of residues involved in ligand recognition and activation of the human A_3 adenosine receptor. *J. Biol. Chem.* **2002**, *277*, 19056−19063.

(33) Colotta, V.; Catarzi, D.; Varano, F.; Melani, F.; Filacchioni, G.; Cecchi, L.; Trincavelli, L.; Martini, C.; Lucacchini, A. Synthesis and A_1 and A_{2A} adenosine binding activity of some pyrano[2,3-*c*]pyrazol-4-ones. *Farmaco* **1998**, *53*, 189−196.

(34) Varani, K.; Merighi, S.; Gessi, S.; Klotz, K.-N.; Leung, E.; Baraldi, P. G.; Cacciari, B.; Romagnoli, R.; Spalluto, G.; Borea, P. A. [^{3}H]-MRE 3008-F20: a novel antagonist radioligand for the pharmacological and biochemical characterization of human A_3 adenosine receptors. *Mol. Pharmacol.* **2000**, *57*, 968−975.

(35) Cheng, Y. C.; Prusoff, W. H. Relation between the inhibition constant K_i and the concentration of inhibitor which causes fifty percent inhibition (IC_{50}) of an enzyme reaction. *Biochem. Pharmacol.* **1973**, *22*, 3099−3108.
(36) OpenMosix: http://www.openMosix.org, 2004.
(37) *MOE (The Molecular Operating Environment)*, version 2005.06; Chemical Computing Group Inc. (1010 Sherbrooke Street West, Suite 910, Montreal, Canada H3A 2R7); http://www.chemcomp.com.
(38) Stewart, J. J. P. *MOPAC 7*; Fujitsu Limited: Tokyo, Japan, 1993.
(39) Palczewski, K.; Kumasaka, T.; Hori, T.; Behnke, C. A.; Motoshima, H.; et al. Crystal structure of rhodopsin: A G protein-coupled receptor. *Science* **2000**, *289*, 739−745.
(40) Cornell, W. D.; Cieplak, P.; Bayly, C. I.; Gould, I. R.; Merz, K. M.; Ferguson, D. M.; Spellmeyer, D. C.; Fox, T.; Caldwell, J. W.; Kollman, P. A. A second generation force field for the simulation of proteins, nucleic acids, and organic molecules. *J. Am. Chem. Soc.* **1995**, *117*, 5179−5196.
(41) Baxter, C. A.; Murray, C. W.; Clark, D. E.; Westhead, D. R.; Eldridge, M. D. Flexible Docking Using Tabù Search and an Empirical Estimate of Binding Affinity. *Proteins: Struct., Funct., Genet.* **1998**, *33*, 367−382.
(42) Halgren, T. Merck molecular force field. I. Basis, form, scope, parameterization, and performance of MMFF94. *J. Comput. Chem.* **1996**, *17*, 490−519.

JM060373W